Cavitation bubble interaction close to ultra-hydrophobic surface

DARINA JASIKOVA, MICHAL KOTEK, MILOS MULLER, VACLAV KOPECKY
Department of Physical Measurement
Technical University of Liberec
Studentska 1402/2 Liberec 1 461 17
CZECH REPUBLIC
darina.jasikova@tul.cz http://cxi.tul.cz

Abstract: - The cavitation bubble has a great potential to be used for local surface hardening. The highly controlled and geometrically placed defined bubbles can easily machine the area of interest modifying the surface of material. However, the effect of pointed pressure hit can be sometimes undesirable. Usage of ultra-hydrophobic cover could shield and spread the force in certain part of working. The aim of this project was to design a setup of Laser Induced Breakup and study the effect of cavitation bubble on ultra-hydrophobic surface. The main interest was focused on the air film behavior that is created on the surface in liquids. Here we used 532nm Nd:YAG pulse laser for the cavitation bubble generation. The process and the impact of cavitation bubble was visualized using high speed shadowgraph.

Key-Words: - Laser Induced Breakdown, Shadowgraph, Cavitation bubble, Hydrophobic Surface

1 Introduction

Cavitation is mainly known for its undesirable effects in turbo machinery; however there is a great potential for its utilization in the industry, medicine, biology, pharmacy, or tissue engineering. The presence of cavitation can cause decrease in turbo machinery efficiency due thrust lowering, increasing of drag force and appearance of additional forces on solid surfaces. Cavities dissolved in vehicle brake system can change the density of the working liquid in an unsuitable moment and thus cause an accident. Finally, the generation of noise and vibration can also indicate the presence of cavitation. The undesirable phenomena associated with cavitation are thermal and mechanical effect during the bubble collapse. It is represented by erosion, mechanical degradation of solids. But in the first few cycles may be acoustic energy of shock waves used for surface hardening in positive way.

The process of cavitation can be generated in any kind of liquid. It is a natural process that can cause many troubles in engineering but on the other hand can be useful. These examples could be disruption of cells, bacteria or viruses, and controlled surface hardening.

The research in the field of cavitation was previously focused mainly on the investigation of bubble behavior in the vicinity of rigid or flexible boundaries; however the current investigations require including the description of response of the impacted material itself. The definition of the material response can help in development of new, more resistant structures or layers which better withstand the action of cavitation bubbles and prolong the service life of products. The key in the understanding of the cavitation interaction with various materials is the investigation of the impact of individual bubbles. The experiments focused on the investigation of the bubble wall interaction can also help to set the physical models which can be effectively used in the modelling of cavitation phenomena at different scales.

Although the current state of technique is at very high level, we are still not able to produce one controllable individual bubble by pressure decrease in the liquid volume, following the cavitation definition. There were found substitute methods to generated cavitation bubble based on point source of heat [1-3]. Anyway, the generation of such bubble is not fully correct in sense of cavitation theory, the bubble behaviour and process of implosion impact towards the surface is the same.

The interaction of the cavitation bubble with surfaces can be influenced by the cavitation itself as well as the surface quality. The key role plays surface roughness, initial hardness, inner stress and surface tension. In response to surface tension arose the question of interfacial behavior of cavitation if the surface is modified.

Nowadays, the main trend in surface modification is the usage of ultra-hydrophobic covers. One of the methods for the ultra-hydrophobic surface covering is using nano-plasma technology [4]. The problem of hydrophobic surfaces is very complex and can be crucial to fluid

mechanics, especially the problem of adhesion of liquid on a solid surface that is set as boundary condition in the most of mathematical models.

The process of ultra-hydrophobic covers could be useful in any phase of surface hardening by influencing the force impact of the bubbles, power distribution over the treated surface. As the cavitation process is stressed concentrating energy into small impacting spot, it produces high pressure peaks. In first case it can be used as a shielding of cavitating bubble impact, or following the observation as the reinforcement element of power transfer.

2 Experimental Methods

The term of cavitation originates from the Latin word *cavea* in a meaning of a hollow place. Generally, cavitation can be defined as collection of effects associated with the formation, occurrence and activity of macroscopic cavities in liquid. The cavities can be void, filled with gas, or vapor, or their mixture. Isolated cavities are often called bubbles. We distinguish several kind of cavitation by physical principle. It can be hydrodynamic, acoustic, optical, or particle cavitation.

There are also methods that enable generation of single cavitation bubble for experimental purposes. All other methods as the spark or laser generated bubbles are closer to the boiling as these are based on the evaporation of small volume of liquid. The bubbles generated by the ultrasonic field satisfy the cavitation definition, however to produce one single bubble is almost impossible.

The one of the method for bubble generation is spark in liquid, or a heated top of a wire. Once the bubble is stable, and of certain volume, it is either over heated, or expose to force impact. The convenient method for generating single cavitation bubble that can be very precisely geometrically placed in the volume of the liquid, and close to the sample, is Laser Induced Breakdown (LIB) [5-8].

The LIB method enables to generate cavitation bubble using ultrashort pulses of milijoules energies. This method is thermal breakdown based on natural plasma generation. This plasma is in form of optical breakdown, if the pulse exposure is from microseconds to femtoseconds' time. There occurs direct, multiphoton, and cascade ionization during the LIB. The significant role plays impurities of the medium, spot size, light wavelength, and pulse width during the breakdown. The whole mechanism of the ionization is very well explained by Kennedy [5].

2.1 Laser Induced Breakdown

The optical breakdown in liquid is usually produced by focusing of the laser light through suitably designed optics. The energy distribution during the growth and collapse of laser induced bubble was described e.g. by Vogel and others in [9, 10]. The authors investigated the influence of the laser pulse duration and input laser energy on the bubble dynamics and the shock waves emission.

Here we chosen green light as exciting light pulse. The absorption coefficient of the 532 nm laser light is only 0.02 m^{-1} in distillated pure water. This wave length requires higher energy input to the system to induce cavitation process. For the single bubble generation we used here the setup for the LIB. The 10 ns short laser pulse was generated using Q-switched Nd: YAG New Wave Gemini pulse laser. This laser worked with one cavity for single shot generation on the wavelength 532 nm. The Q-switch signal synchronized the high speed camera running in triggering mode.

The optical setup was based on plano-convex mirror for focusing of laser light into the plasma spot instead of the plano-convex lens. The schema of this setup is seen in Fig. 1.

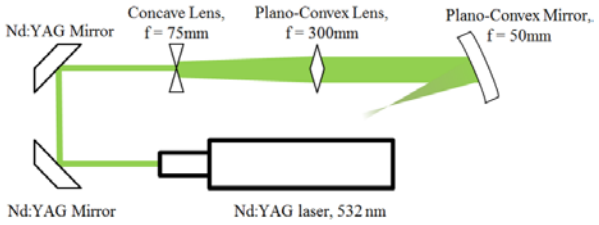

Fig. 1 Experimental setup of the reverse focusing optical setup

The energy of the laser beam was adjusted and measured with Ophir pyroelectric energy sensor. We measured the laser energy in three positions. There is seen the characteristic of laser light energy calibrated to the position of attenuator. NewWave Gemini laser enables setting of light intensity adjusting flash lamp power and fine adjustment using attenuator. The attenuator enables controllable backward loop, as an actual value is seen on the display. According to the energy calibration we did the "bubble size - laser energy" calibration to predict the final bubble sizes. There is an optical setup dependent on prediction of the bubble size – long distance microscope extension, optimal field of view and illuminating system position.

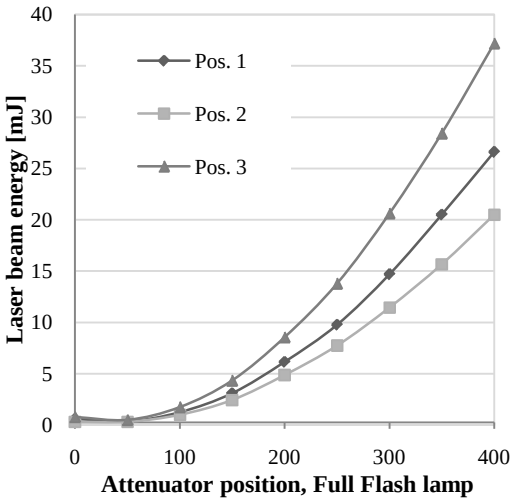

Fig. 2 The energy of laser beam measured in three positions to obtain the losses caused by optics; Position 1 was at the outcome of the laser head, position 2 was after the collimating lens, and position 3 was after the focusing mirror

The dataset of at least 20 cavitation processes for statistic evaluation was captured. This maximum bubble size was detected in each image and it was related to the energy of the laser beam. The bubble size was measured in vertical and horizontal axis and the final value represents the average value. The increase of the laser energy causes the increase of horizontal value of cavitation bubble size. This effect corresponds with the temporal and spatial plasma evolution at the very beginning of the process.

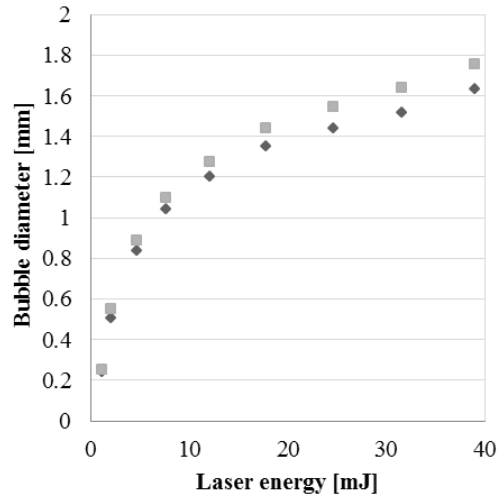

Fig. 3 Cavitation bubble diameter on the input laser energy in water on 532nm

The relation between the energy of the laser beam and the cavitation bubble size is asymptotic. This means that further increase of laser energy does not lead to significant increase of the bubble size. According to Kennedy [9], the plasma temperature shows asymptotic dependence on the laser pulse energy as well. With higher laser energy we recognized the negative influence of impurities and presence of segmentations on the bubble surface

2.2 Samples Preparation

We prepared a set of samples for purpose of the study of cavitation bubble effect on the ultra-hydrophobic surface. The matrix material was polycarbonate (PCB), polypropylene (PP), and glass as a reference sample. All samples were spray coated with nanopolymeric UltraEverDry®, and cold Ar+O^2 plasma treated.

The plasma deposition includes a wide range of specific technologies, which differ from each other as technological equipment and working conditions, as well as the achieved results, i.e. the types and composition of the various deposits and their properties, structure, and chemical composition. Only some of them exhibit nanostructured character.

The one way of making nanostructured thin films especially with varying degrees of hydrophobicity of the above plasma jet systems. Using the plasma jet at atmospheric pressure for a modification of macromolecular materials and surfaces is disclosed in EP 07466017.6-1226 (Klima, M. et al. 2007). The plasma jet generates plasma at atmospheric pressure and is based on principle of the hollow cathode running with high frequency (13.56 MHz).

The first set of samples was designed to cover the influence of the contact angle on the cavitation bubble behavior. There were prepared samples of PCB with contact angle (CA) 110° (Sample A), CA 150° (Sample B), and CA 160° (Sample C). Sample A with ultra-hydrophobic layer obtained by direct deposition of HMDSO precursor of argon plasma generated by plasma jets.

Sample B and C were prepared by the plasma, and the precursor formed HMDSO ultra hydrophobic layers, subsequently it was applied to two different types according nanopolymer sample (to improve stability and mechanical properties). For sample B was used nanopolymer based on SiO^2 in ethanol solution (classical Nano-glass) for sample B was chosen based nanopolymer fluoro hydrocarbons in aqueous solution (rubbed into the structure ultra-hydrophobic layer).

There were prepared samples of various matrix materials (PP, PCB, and PE) with application of the most resistant ultra-hydrophobic cover for the second part of experiments. The very resistant covers were fluoro hydrocarbons.

2.3 Visualization methods

We used shadowgraphy setup for the bubble visualization. This setup consists of continuous LED matrix daylight lamp Veritas, MiniConstellation 120 – 5000 K of illuminance 92 klux in 0.5 m, equipped with optical diffuse filter. Opposite to the light source high speed CMOS camera SpeedSense was placed. This camera is working on frequency 180 kHz with spatial resolution of (128 x 128) px or lower frequency with higher resolution up to (1280 x 800) px, and the dynamic range 12 bit. The camera exposure time was to 1 μs.

The camera was mounted with optical lens system INFINIPROBE™ TS-160 universal macro/micro imaging system that enables 4x, and 16x magnification. The lens was fitted with edge pass and long pass filter cut-on wavelength 550 nm low pass optical filter to reduce the backward laser flashes to the camera and also to eliminate the flash generated while plasmatic breakdown.

The camera was running in the triggering mode. The trigger was activated with the Q-switch pulse of laser. Once the motion was captured it dataset was moved to computer. The beginning point of the synchronization was the plasma spot accompanied by the flash. The experimental setup is seen in Fig. 3.

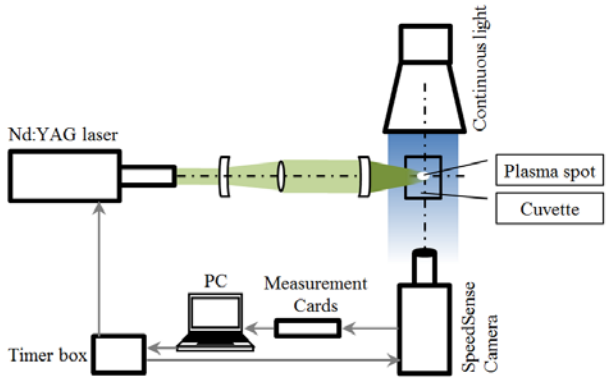

Fig. 3 The experimental setup for generation of cavitation bubble and illuminating system for high speed shadowgraph method

3 Results and Discussion

The interaction between the liquid and ultra-hydrophobic surface is followed by evolution of continuous layer of air - air film. The presence of the air film is theoretically supported by Cassie-Baxter's theory of contact angle [13]. This effect can be observed as the sample is dip in water, and the air film is seen as a reflecting layer. The quality and the consistency of air film depend on the quality of layer, contact angle, and surface roughness. The presence of air film is essential in our further experiments with cavitation bubble.

3.1 Estimation of air film

There has been set the laboratory device for testing the air film in the first part of our research. The method was based on the knowledge of micro PIV visualizations. Here we used industrial Jai camera with 5.5Mpix resolution and laser illuminating system [11, 12]. There were prepared special testing samples covered with hydrophobic surface and designed to ensure the optical access. The experimental sample setup was joined to hydraulic circuit for study of the effect of liquid flow on the behaviour of the air film. The liquid flow is represented by Reynolds number. The aim of this part of research was established the critical Reynolds number under which the air film is present. The result of this study was summary graph of the static contact angle effect on quality of air film and its dependence on Reynolds number (Fig. 4).

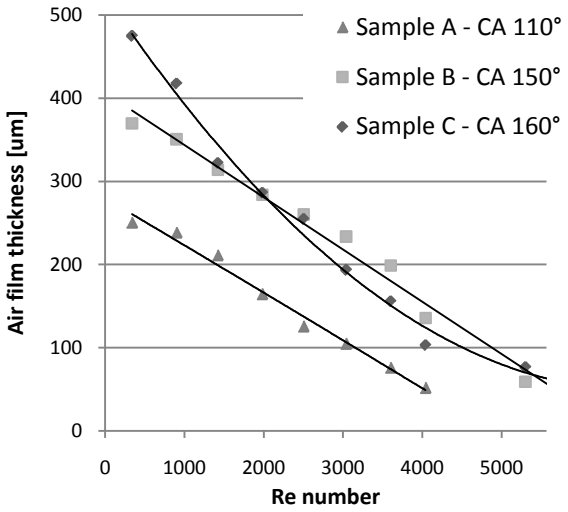

Fig. 4 Air film thickness experimentally established depending on the Reynolds number

We can read from the Fig. 4 that the air film thickness is strongly dependent on the initial quality that is represented with the static contact angle. The surface with the highest contact angle (160°) based on fluoro hydrocarbons nanopolymers is highly resistant to dynamic of liquid flow. The maximal Reynolds number that was reached as the air film was still fluoro hydrocarbons was 5600.

3.2 Visualization of cavitation bubble

We were interested of the cavitation bubble interaction with the air film formed on the hydrophobic surface in the second part of our experimental work. The great advantage of LIB generated cavitation bubble is its space orientation to the investigated sample. The bubble can be precisely placed in the space in various distances.

The most common setup is derivate from the bubble maximal size, and the major impact force is expected on 1D, or 1R of cavitation bubble. Here we present the result for 1D bubble size visualization in relation to behaviour of the air film on the ultra-hydrophobic surface [14]. The maximal size of the cavitation bubble can be also precisely regulated by the input laser energy. Here we used the cavitation bubble of maximal size 1mm that corresponds to 10 mJ of input laser energy.

The cavitation tests in cuvette run in 10 shots regime. The comparison of the shots and be seen in Fig. 5. The cavitation process was captured synchronously and pictures presented here are sort by the time of the cavitation process phase and for each shot. There are selected 3 fundamental changes, for the 1st, 5th and 10th laser shot and cavitation bubble impact. There are seen changes on the air film quality. There were selected a glass sample as a reference with static contact angle 60°. There is no presence of air film, or the bubbles on the surface.

The sample B with contact angle 110° formed separated bubbles on the surface. We placed the cavitation bubble above this sessile bubble to observe interaction between these two. The sessile bubble shrunk after each cavitation impact and after 10 runs it became more bordered and focused.

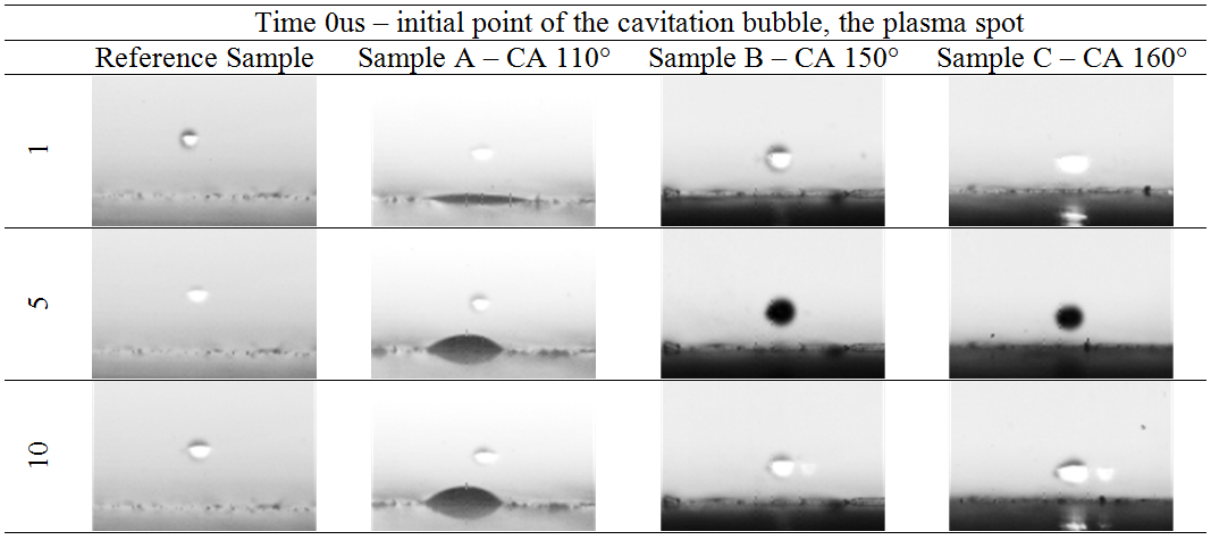

Fig. 5 The cavitation process at the initial point of plasma spot generation

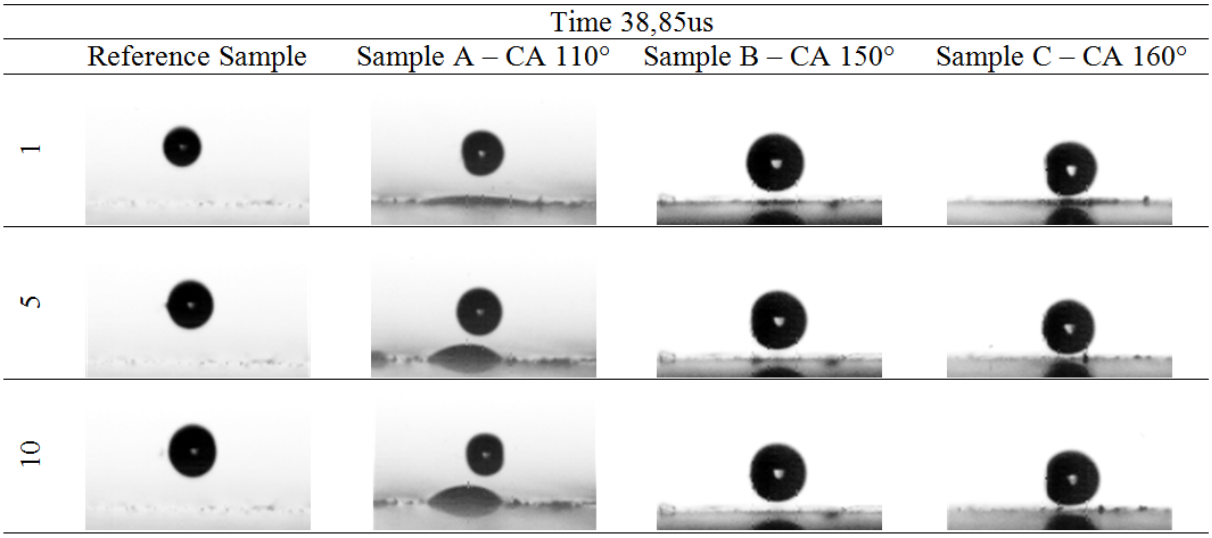

Fig. 6 Fully developed cavitation bubble of maximal size at time 38.85us from the very start of the process

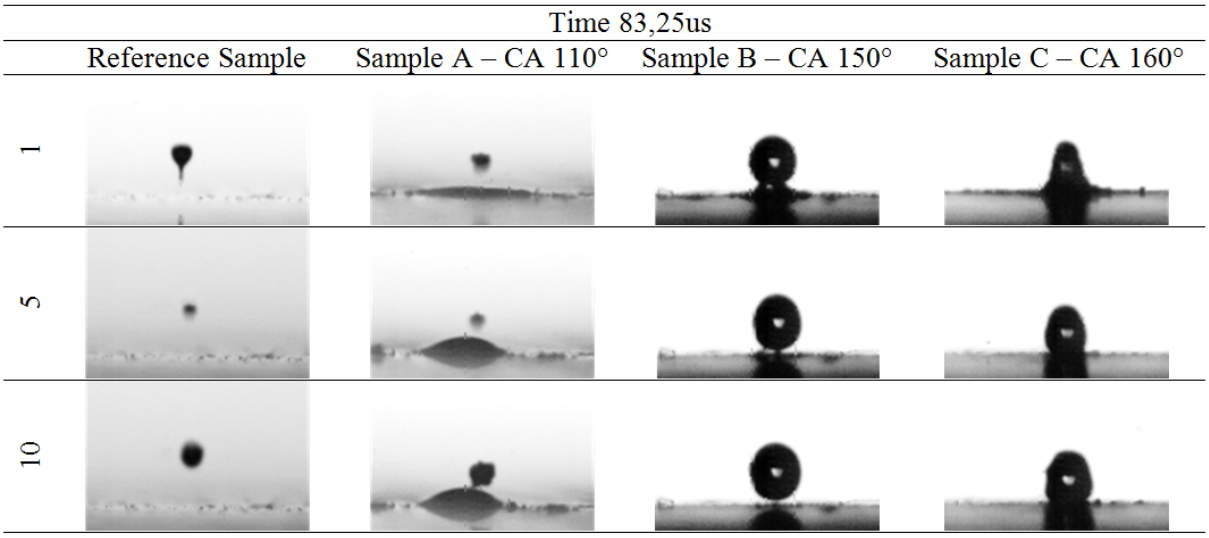

Fig. 7 Cavitation bubble impacting the solid wall at time 83.25us from beginning of the process

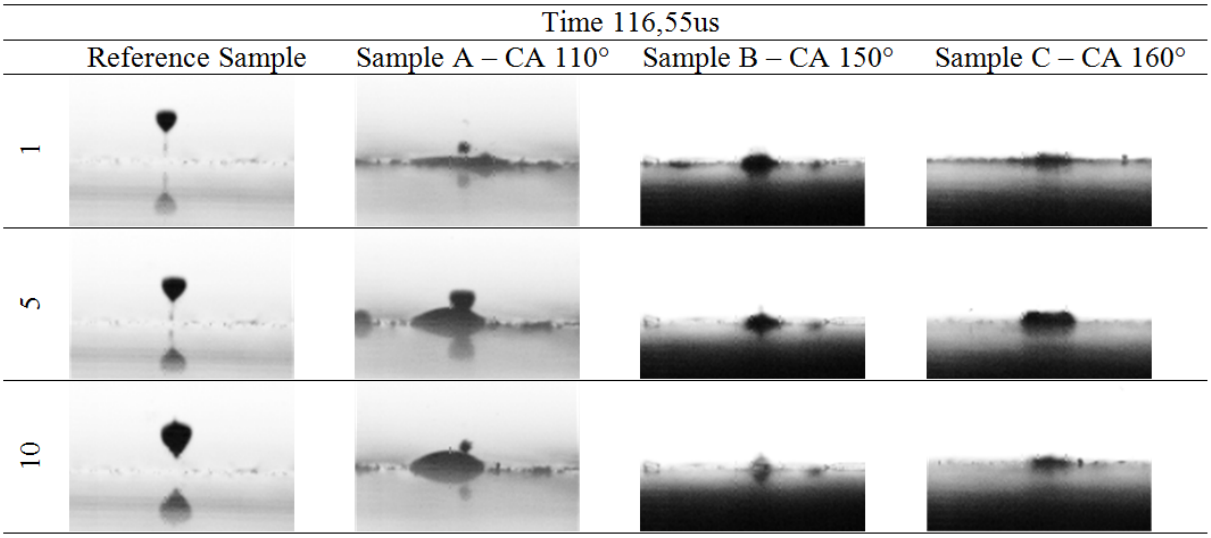

Fig. 8 Cavitation bubble implosion and surface interaction at time 116.55us from beginning of the process

There is seen fully developed cavitation bubble at time 38.85 us timed from the plasma spot as the beginning of the process. The cavitation bubble starting interaction with the air film at time 83.25us. There is seen the air film approach towards the cavitation bubble. This time is just before the cavitation bubble implosion. The air film is very strong affected due the reverse forces acting towards the bubble

The cavitation bubble generates the thing jet stream at the time 116.55us from plasma spot. There is a great pressure impact on the surface during this phase. The surface is interfered and there can be also measured great force impact. There is seen a big movement of the sessile drop as it is acted by cavitation bubble. The air film reacts in the opposite way and the pointed pressure impact is distributed over the air film surface. The background material is protected against the focused force impact, but the force is spread over the greater area. The interesting effect of the air film behaviour is sudden movement towards the cavitation bubble. This movement could be induced by the shock wave that is amplified over the volume of liquid. The air film keeps oscillating for the next at least 200us.

The results were obtained through the financial support of LO1201 under the Ministry of Education, Youth and Sports in the framework of the targeted support of the “National Programme for Sustainability I”. Authors also acknowledge the support of TH01020982 project named “Efficiency improvement of energy storage and ensuring grid stability by extending the operating range of pumped storage”, and the institutional support Faculty of Mechatronics, Informatics and Interdisciplinary Studies of Technical University of Liberec.

4 Conclusion

The interaction of the cavitation bubble and the air film generated on the ultra-hydrophobic surface is noticeable on the geometry 1D – the bubble is in the distance one diameter bubble maximum size far from the surface. There can be seen significant effect of the air film attraction towards the cavitation bubble during the collapse phase of the cavitation process. The following impact force is absorbed with the air film and distributed over the air film area. This effect increases the cavitation bubble impact radius up to 7D. The shockwave spreads over the air film and can be observed as oscillating pattern. The energy transmitted from the cavitation bubble to the air film is not absorbed immediately.

We also tested the repeatable generated cavitation bubbles and their effect on air film. The geometry was set as well as the distance between the bubble and surface. There was observed negative influence on the air film just after the first 5 cavitation bubbles. During the next cavitation process the air film was reduced. The effect of 10 cavitation bubbles is still reversible. There has been observed decrease of the static contact angle in the impacting area on the surfaces just after the cavitation process exposure. After drying the surface recovered.

The progressive erosion caused by cavitation bubble also further influencing the ultra-hydrophobic surface. The damaged ultra-hydrophobic treatment works no more. This regime is irreversible.

We have also tested the ultra-hydrophobic surface that creates surface separated bubble in the contact with fluid (Sample Glass-A). The cavitation process was set above the surface bubble and it was observed the reducing of the surface bubble till it definitively disappeared.

The great potential and proposal for the further study is a measurement of impact force over the sample. Once is proved the hardening effect in spread area this result could improve the methodic of laser ablation, or ultrasonic cavitation hardening just removing the local tension incensement that is undesirable.

References:

[1] W. Lauterborn, T. Kurz, R. Mettin, P. Koch, D. Kroninger, D. Schanz, Acoustic cavitation and bubble dynamics, *Archives of Acoustics*, 33, 2008, 609-617.

[2] M. Müller, W. Garen, S. Koch, F. Marsik, W. Neu and E. Saburov, Shock Waves and Cavitation Bubbles in Water and Isooctane generated by Nd:YAG Laser, Experimental and Theoretical Results, *Proc. SPIE*, 5399, 2004, 275-282.

[3] D. Frost, B. Sturtevant, Effect of Ambient Pressure on the Instability of a Liquid Boiling Explosively at the Superheat Limit, *Transactions of the ASME*, 108, 1986, 418-424.

[4] M. Klima, et al., The Method of Making a Physically and Chemically Active Enviroment by Means of a Plasma jet and the Related Plasma Jet, US 6.525.481 (2003), EP 1077021 (2005), 1998.

[5] P. K. Kennedy, D. X. Hammer, B. A. Rockwell, Laser-induced breakdown in aqueous media, *Progress in Quantum Electronics*, 21 (3), 1997, 155-248.

[6] A. De-Bosset, D. Obreschkow, P. Kobel, M. Farhat, Direct effects of gravity on cavitation bubble collapse, *Proceedings of the 58 international astronautical congress*, 2007, 1–5.

[7] D. Obreschkow, M. Tinguely, N. Dorsaz, P. Kobel, A. Bosset, M. Farhat, The quest for the most spherical bubble: experimental setup and data overview, *Experiments in Fluids*, 54, 2013, 1503.

[8] A. Shima A., Y. Tomita, The behavior of a spherical bubble near a solid wall in a compressible liquid, *Ingenieur-Archiv* 51, 1981, 243-255.

[9] A. Vogel, et al., Energy balance of optical breakdown in water at nanosecond to femtosecond time scales, *Applied Physics B: Lasers and Optics* 68, 1999, 271-280.

[10] E. A. Brujan, K. Nahen, P. Schmidt, A. Vogel, Dynamics of laser-induced cavitation bubbles near elastic boundary, *J.Fluid Mech.* 433, 2001, 251-281.

[11] D. Jasikova, M. Kotek, S. Fialova, V. Kopecky, A liquid interaction with ultrahydrophobic surfaces, *EPJ Web of Conferences*, 114, 2016, 1-6.

[12] D. Jasikova, M. Kotek, V. Kopecky, An effect of entrance length on development of velocity profile in channel of millimeter dimensions, *AIP Conf. Proc.*, 1745, 2016, 1-6.

[13] A., B., D. Cassie, S. Baxter, Wettability of porous surfaces, *Transactions of the Faraday Society*, 40, 1944, 546-551.

[14] D. Jasikova, M. Muller, M. Kotek, V. Kopecky, The study of single cavitation bubble generated with LIB technique and its force impact on the solid wall, *International Journal of Mechanics*, 9, 2015, 76-82.